To be Submitted to the 29th International Conference on High-Energy Physics ICHEP98,
Vancouver, Canada, July 1998

A Search for Squarks of R-Parity Violating SUSY at HERA

H1 Collaboration

Abstract

A search for squarks of R-parity violating supersymmetry is performed in ep collisions at HERA using H1 1994$\rightarrow$1997 data corresponding to an integrated luminosity of 37 pb $^{-1}$. Direct single production of squarks of each generation by e^{+}-quark fusion via a Yukawa coupling λ' is considered and various possible R-parity violating decays and gauge decays of the squarks are taken into account. Such couplings could lead in particular to leptoquark-like final states or to explicit manifestation of lepton number violation. The sensitivity to λ' is shown to be only weakly dependent on the free parameters of the Minimal Supersymmetric Standard Model and the reach in the mass-coupling plane extends to domains unexplored in other direct or indirect searches. For a Yukawa coupling of the electromagnetic strength squark masses up to 262 GeV can be excluded at the 95% confidence level; this sensitivity reaches still 175 GeV for a 100 times smaller coupling strength. Squarks coupling to both $e-q$ and $\tau-q'$ pairs are also searched for and the absence of signal allows constraints to be set on the Yukawa coupling involving the τ lepton which explore a yet uncovered domain.

Abstract: 580
Parallel sessions: 10
Plenary sessions: 12

1 Introduction

The ep collider HERA which provides both baryonic and leptonic quantum numbers in the initial state is ideally suited to search for new particles possessing couplings to an electron-parton pair. Such particles could be squarks, the scalar supersymmetric (SUSY) partners of the quarks, in SUSY models where R-parity is violated ($\not{R}_p$) via Yukawa couplings λ'. These squarks could thus be resonantly produced at HERA, via the fusion of the $E_e^0 = 27.5$ GeV initial state positron with a quark coming from the $E_p^0 = 820$ GeV incident proton, up to the kinematic limit of $\sqrt{s} \simeq 300$ GeV.

In 1996, both H1 [1] and ZEUS [2] collaborations reported an excess of events at very high Q^2 (i.e. very high energy of the scattered positron), above the expectation of Standard Model (SM) Neutral Current (NC) Deep Inelastic Scattering (DIS). This relied in H1 on $\simeq 14$ pb $^{-1}$ of e^+p data collected between 1994 and 1996. This and the apparent "clustering" of the H1 events at invariant masses of $\simeq 200$ GeV, although not supported by ZEUS observations [3, 4], has enhanced the interest in theories beyond the SM which could possibly provide an interpretation of the excess involving the s-channel resonant production of a new particle such as a leptoquark or a squark in $\not{R}_p$ SUSY [5]. The mass range accessible for direct production of leptoquarks at HERA is now severely contrained by the recent results of the TeVatron experiments [6, 7] which restrict first generation leptoquark masses at 95% confidence level (CL) to $M \gtrsim 240$ GeV ($M \gtrsim 200$ GeV) [8] for a branching ratio β_{eq} of the new particle into $e + q$ of 1 ($\gtrsim 0.5$). $\not{R}_p$ SUSY provides a framework in which β_{eq} can be naturally small given the competition with gauge decay modes of the squarks, and thus leptoquark-like TeVatron constraints can be easily avoided. This strongly emphasizes the necessity [5] to perform systematic searches for squarks covering both $\not{R}_p$-decay modes and various possible gauge decay modes.

In this paper, squarks are searched through single production via a $\not{R}_p$ coupling, considering both $\not{R}_p$ decays and decays via gauge couplings involving mixed states of gauginos and higgsinos. The analysis uses the 1994 $\rightarrow$ 1997 e^+p data corresponding to an integrated luminosity of 37 pb $^{-1}$. This represents an increase of statistics of a factor ~ 13 compared to earlier $\not{R}_p$-violating squark searches at HERA [9, 10].

2 Phenomenology

The most general SUSY theory which preserves gauge invariance of the Standard Model (SM) allows for Yukawa couplings between one scalar squark ($\tilde{q}$) or slepton ($\tilde{l}$) and two known SM fermions. Such couplings induce violation of the R-parity defined as $R_p = (-1)^{3B+L+2S}$, where S denotes the spin, B the baryon number and L the lepton number of the particles. We consider here the SUSY phenomenology at HERA in presence of $\not{R}_p$ Yukawa couplings but maintaining otherwise the minimal field content of the so-called Minimal Supersymmetric Standard Model (MSSM). Of special interest for HERA are those Yukawa vertices which couple a squark to a lepton-quark pair. These are described in the superpotential by the terms $\lambda'_{ijk} L_i Q_j \bar{D}_k$, with i, j, k being generation indices [1]. The corresponding part of the Lagrangian, expanded in fields, reads as [11] :

$$\begin{aligned} \mathcal{L}_{L_i Q_j \bar{D}_k} &= \lambda'_{ijk} \Big[-\tilde{e}^i_L u^j_L \bar{d}^k_R - e^i_L \tilde{u}^j_L \bar{d}^k_R - (\bar{e}^i_L)^c u^j_L \tilde{d}^{k*}_R \\ &\quad + \tilde{\nu}^i_L d^j_L \bar{d}^k_R + \nu_L \tilde{d}^j_L \bar{d}^k_R + (\bar{\nu}^i_L)^c d^j_L \tilde{d}^{k*}_R \Big] + \text{h.c.} \end{aligned}$$

[1] In the usual superfields notation, L_i, Q_j and $\bar{D}_k$ contain respectively the left-handed lepton doublet, quark doublet and the right handed quark singlet.

where the superscripts ^{c} denote the charge conjugate spinors and the * the complex conjugate of scalar fields. Hence, with an e^+ in the initial state, the couplings λ'_{1jk} allow for resonant production of squarks through $e-q$ fusion. For the nine possible λ'_{1jk} couplings, the corresponding single production processes are given in table 1. The $\tilde{u}^j_L$ ($\tilde{d}^{k*}_R$) production cross section approx-

λ'_{1jk}	production process	
111	$e^+ + \bar{u} \to \tilde{d}^*_R$	$e^+ + d \to \tilde{u}_L$
112	$e^+ + \bar{u} \to \tilde{s}^*_R$	$e^+ + s \to \tilde{u}_L$
113	$e^+ + \bar{u} \to \tilde{b}^*_R$	$e^+ + b \to \tilde{u}_L$
121	$e^+ + \bar{c} \to \tilde{d}^*_R$	$e^+ + d \to \tilde{c}_L$
122	$e^+ + \bar{c} \to \tilde{s}^*_R$	$e^+ + s \to \tilde{c}_L$
123	$e^+ + \bar{c} \to \tilde{b}^*_R$	$e^+ + b \to \tilde{c}_L$
131	$e^+ + \bar{t} \to \tilde{d}^*_R$	$e^+ + d \to \tilde{t}_L$
132	$e^+ + \bar{t} \to \tilde{s}^*_R$	$e^+ + s \to \tilde{t}_L$
133	$e^+ + \bar{t} \to \tilde{b}^*_R$	$e^+ + b \to \tilde{t}_L$

Table 1: Squark production processes at HERA (e^+ beam) via a R-parity violating λ'_{1jk} coupling.

imately scales as $\lambda'^2_{1jk} \times d^k(x)$ ($\bar{u}^j(x)$) where $d^k(x)$ ($\bar{u}^j(x)$) are probabilities to find a quark d^k ($\bar{u}^j$) in the proton with a momentum fraction $x = M^2_{\tilde{q}}/s$; $M_{\tilde{q}}$ denotes the squark mass and $\sqrt{s}$ is the available energy in the ep centre of mass frame. With an e^+ incident beam, HERA is best sensitive to couplings λ'_{1j1}, where mainly $\tilde{u}^j_L$ squarks could be produced via processes involving a valence d quark. On the contrary, future HERA e^-p data will allow to better probe couplings λ'_{11k} and $\tilde{d}^k_R$ squarks.

In this paper, squarks are searched under the simplifying assumptions that:

- the lightest supersymmetric particle (LSP) is the lightest neutralino χ^0_1;
- gluinos are heavier than the squarks such that decays $\tilde{q} \to q + \tilde{g}$ are kinematically forbidden;
- either one of the λ'_{1jk} dominates, or one product of couplings $\lambda'_{1jk} \times \lambda'_{3jl}$ is non-vanishing. This latter possibility, leading to lepton flavor violation processes, is addressed independently in the last part of this paper.

The squarks decay either via their Yukawa coupling into SM fermions, or via their gauge couplings into a quark and a neutralino χ^0_i ($i = 1, 4$) or a chargino χ^+_j ($j = 1, 2$). The mass eigenstates χ^0_i and χ^+_j are mixed states of gauginos and higgsinos and are in general unstable. This latter point holds in $\not{R}_p$ SUSY also for the LSP which decays via λ'_{1jk} into a quark, an antiquark and a lepton [11]. This is in contrast to the MSSM and has important phenomenological and possibly cosmological consequences.

In cases where both production and decay occur through a λ'_{1jk} coupling (e.g. Fig. 1a and c for $\lambda'_{111} \neq 0$), the squarks behave as scalar leptoquarks [12]. The $\tilde{d}^{k*}_R$ can decay either into $e^+ + \bar{u}^j$ or $\nu_e + \bar{d}^j$ while the $\tilde{u}^j_L$ only decays into $e^+ + d^k$ by gauge invariance. Hence, the final state signatures consist of a lepton and a jet and are, event-by-event, indistinguishable from the SM neutral and charged current DIS.

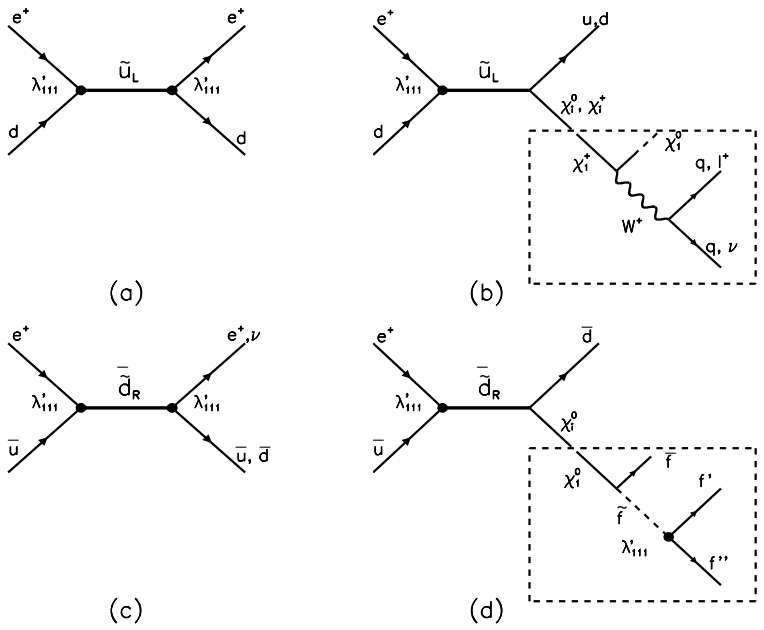

Figure 1: Lowest order s-channel diagrams for first generation squark production at HERA followed by (a),(c) $\not{R}_p$ decays and (b),(d) gauge decays. In (b) and (d), the emerging neutralino or chargino might subsequently undergo $\not{R}_p$ decays of which examples are shown in the dashed boxes for (b) the χ_1^+ and (d) the χ_1^0.

In cases where the $\tilde{u}_L^j$ (resp. $\tilde{d}_R^{k*}$) undergoes a gauge decay into a χ_α^0 or a χ_β^+ (resp. χ_α^0), (e.g. Fig. 1b and d) the final state will depend on the subsequent decay of the χ. Neutralinos can undergo the $\not{R}_p$ decays $\chi_\alpha^0 \to e^\pm q\bar{q}'$ or $\chi_\alpha^0 \to \nu q\bar{q}$, the former (latter) being dominant if χ_α^0 is dominated by its photino (zino) component. When χ_α^0 decays via $\not{R}_p$ into a charged lepton, both the "right" and the "wrong" sign lepton (compared to incident beam) are equally probable leading to largely background free striking signatures for lepton number violation. On the contrary, the only $\not{R}_p$ decays for charginos are $\chi_\alpha^+ \to \nu u^j \bar{d}^k$ and $\chi_\alpha^+ \to e^+ d^k \bar{d}^j$. Neutralinos χ_α^0 with $\alpha > 1$ as well as charginos can also undergo gauge decays into a lighter χ and two SM fermions, through a real or virtual gauge boson or sfermion.

Finally, the possible decay chains of the $\tilde{u}_L^j$ and $\tilde{d}_R^{k*}$ can be classified into eight distinguishable event topologies, labelled S1 to S8 in [10]. This classification relies on the number of charged leptons and/or jets in the final state, and on the presence of missing energy. The relative contributions of each of these decay channels depend on the value of the Yukawa coupling λ'_{1jk} and on the gaugino-higgsino mixture of neutralinos and charginos. This is discussed in more detail in [10, 13, 14, 15]. In general, gauge decays contribute strongly at low χ_1^0 masses and small Yukawa couplings.

In this paper, we concentrate on decay channels S1 to S4. Table 2 describes the four final states analysed here, and gives example decay patterns in each case. As mentioned before, a complementary search, assuming that two $\not{R}_p$ couplings λ'_{1jk} and λ'_{3jl} are non-vanishing and dominate all other λ', has also been carried out and is presented in the last part of this paper. In this case, squarks produced via λ'_{1jk} are assumed to undergo $\not{R}_p$ decays only, via λ'_{1jk} or λ'_{3jl} leading respectively to $e + jet$ or $\tau + jet$ final states. This analysis of $\tau + jet$ topologies, restricted here to hadronic decays of the τ, is carried out for the first time in H1 experiment. The case of a non-vanishing product $\lambda'_{1jk} \times \lambda'_{2jl}$, which could allow for $e^+q \to \tilde{q} \to \mu^+ + q'$ processes, is not considered in this paper. Leptoquark searches reported in [16] have shown that no $e^+p \to \mu^+ + jet + X$ candidate compatible with the two-body decay of an s-channel resonance is observed in all available data.

Channel	Decay processes	Signature
S1	$\tilde{q} \xrightarrow{\lambda'} e^+ \; q'$	High P_T e^+ + 1 jet
S2	$\tilde{d}^*_R \xrightarrow{\lambda'} \nu_e \; \bar{d}$	Missing P_T + 1 jet
S3	$\tilde{q} \longrightarrow q \; \chi^0_\alpha$, $\chi^0_\alpha \xhookrightarrow{\lambda'} e^+\bar{q}'q''$; $\tilde{u}_L \longrightarrow d \; \chi^+_\alpha$, $\chi^+_\alpha \xhookrightarrow{\lambda'} e^+ d\bar{d}$; $\tilde{u}_L \longrightarrow d \; \chi^+_\alpha$, $\chi^+_\alpha \hookrightarrow W^+\chi^\beta_1$, $W^+ \xhookrightarrow{\lambda'} e^+\bar{q}'q''$, $W^+ \hookrightarrow q \; \bar{q}'$	High P_T e^+ + multiple jets
S4	$\tilde{q} \longrightarrow q \; \chi^0_\alpha$, $\chi^0_\alpha \xhookrightarrow{\lambda'} e^-\bar{q}'q''$; $\tilde{u}_L \longrightarrow d \; \chi^+_\alpha$, $\chi^+_\alpha \hookrightarrow W^+\chi^0_\beta$, $W^+ \xhookrightarrow{\lambda'} e^-\bar{q}'q''$, $W^+ \hookrightarrow q \; \bar{q}'$	High P_T e^- (i.e. wrong sign lepton) + multiple jets

Table 2: Squark decay channels in $R\!\!\!/_p$ SUSY classified per distinguishable event topologies. Only the final states which are analysed here are listed in the table. The list of processes contributing to a given event topology is here representative but not exhaustive, e.g. the gauge decays of the χ^+_α involving a virtual W^+ (Fig. 1b) may also proceed via a virtual sfermion.

3 The H1 detector

A detailed description of the H1 detector can be found in [17]. Here we describe only the components relevant for the present analysis in which the final state of the events involves either a positron[2] with high transverse energy or a large amount of hadronic transverse energy flow.

The positron energy and angle are measured in a liquid argon (LAr) sampling calorimeter [18] covering the polar angular[3] range $4° \leq \theta \leq 154°$ and all azimuthal angles. The granularity is optimized to provide fine and approximately uniform segmentation in laboratory pseudorapidity and azimuthal angle ϕ. It consists of a lead/argon electromagnetic section followed by a stainless steel/argon hadronic section. Electromagnetic shower energies are measured with a resolution of $\sigma(E)/E \simeq 12\%/\sqrt{E/\text{ GeV}} \oplus 1\%$ and pion induced hadronic energies with $\sigma(E)/E \simeq 50\%/\sqrt{E/\text{ GeV}} \oplus 2\%$ after software energy weighting. These resolutions were measured in test beams with electron energies up to 166 GeV [19, 20] and pion energies up to 205 GeV [20]. The absolute energy scales are known to 3% and 4% for electromagnetic and hadronic energies respectively. The angular resolution on the positron measured from the electromagnetic shower in the calorimeter varies from ~ 2 mrad below 30° to $\lesssim 5$ mrad at larger

[2]Unless otherwise stated, the analysis does not distinguish explicitly between e^+ and e^-.

[3]The z axis is taken to be in the direction of the incident proton, and the origin of coordinates is the nominal ep interaction point.

angles. A lead/scintillating-fibre backward calorimeter [21] extends the coverage[4] at larger angles ($153^\circ \leq \theta \lesssim 178^\circ$).

Located inside the calorimeters is the tracking system which is used here to determine the position of the interaction vertex. The main components of this system are central drift and proportional chambers ($25^\circ \leq \theta \leq 155^\circ$), a forward track detector ($7^\circ \leq \theta \leq 25^\circ$) and a backward drift chamber[3]. The tracking chambers and calorimeters are surrounded by a superconducting solenoid providing a uniform field of 1.15 T parallel to the z axis within the detector volume. The instrumented iron return yoke surrounding this solenoid is used to measure leakage of hadronic showers and to recognize muons. The luminosity is determined from the rate of Bethe-Heitler $ep \to ep\gamma$ bremsstrahlung events measured in a luminosity monitor. This consists of a positron tagger (e-tagger) and a photon tagger (γ-tagger), located -33 m and -103 m respectively from the interaction point, respectively.

The increase of statistics accumulated in 1997 allowed for the first time to perform an *in situ* calibration of the electromagnetic section of the LAr calorimeter exploiting [23] the kinematic constraints of NC DIS and elastic QED Compton events. The large amount of data with a lepton scattered in the central wheels of the LAr allowed a very fine calibration in this region leading to a precision of 1% for θ between 80° and 150° on the electromagnetic energy scale. Moreover, in the forward region of the LAr calorimeter, the calibration scale has globally been improved and it was verified that the absolute calibration of positron energies ranges within the $\pm 3\%$ systematics originally estimated from extrapolations based on CERN test beam results. The analysis described in the following relies on this updated calibration.

4 Monte Carlo Event Generators

A complete Monte Carlo simulation of the H1 detector response is performed for each possible background source.

For the NC or CC DIS background estimates we use of the DJANGO [24] event generator, which includes first order QED radiative corrections. Simulation of real bremsstrahlung photons, based on HERACLES [25], is also included. QCD radiation at all orders is treated following the approach of the Color Dipole Model [26] and are implemented using ARIADNE [27]. The hadronic final state is generated using the string fragmentation model [28]. For DIS at high Q^2, in the range relevant for S1 topology, several samples of events have been simulated, each amounting to at least 10 times the available integrated luminosity. In particular, the statistics simulated for the tail of the Q^2 distribution above 10000 GeV^2 corresponds to $\simeq 1500$ times that of the data. For NC DIS at medium Q^2, which constitutes an important part of the SM background for S3 topology, a sample of $\simeq 3$ times the integrated luminosity of the data has been used. The parton densities in the proton used to estimate DIS expectations are taken from the MRS H [29] parametrization.

For the direct and resolved photoproduction of light and heavy flavours, we use the PYTHIA MC event generator [31] which relies on first order QCD matrix element and uses leading-log parton showers and string fragmentation [28]. The GRV LO (GRV-G LO) parton densities [32] in the proton (photon) are used at low Q^2. The statistics simulated amounts to at least 3 times that of the data.

[4]The detectors in the backward region were upgraded in 1995 by the replacement of the lead/scintillator tile calorimeter [22] and a proportional chamber.

The simulation of the leptoquark-like signatures (S1 and S2 topologies) relies on the event generator LEGO [33] which is described in more detail in [34]. For squarks undergoing gauge decays leading to $e^{\pm}$ and multiple jets final states (topologies S3 and S4), the event generator SUSSEX [33] based on the cross sections given in [11] is used. In both LEGO and SUSSEX initial state bremsstrahlung in the collinear approximation is simulated, initial and final state parton showers are simulated following the DGLAP evolution, and string fragmentation [31, 28] is used for the non-perturbative part of the hadronization. The parton densities used [29] are evaluated at the scale of the new particle mass. This scale is also chosen for the maximum virtuality of parton showers. In the SUSSEX generator however, the parton showers modelling QCD radiation off the two quarks emerging from the χ decay are started at a scale given by the χ mass.

Several samples of events corresponding to final states S1 to S4 have been generated and were passed through a complete simulation of the H1 detector. The squark mass for these simulations has been varied from 50 GeV to 275 GeV in steps of $\simeq 25$ GeV. For gauge decays of squarks, the χ mass ranges between 40 GeV and 160 GeV.

5 Analysis

5.1 Selection of ep collisions

The data reduction starts by the rejection of non-colliding background. It is common to all channels presented below and requires that the event survives a set of halo and cosmic muon filters, and that it is properly in time relative to interacting bunch crossings. Moreover, a primary interaction vertex must be reconstructed in the range $\mid z - \bar{z} \mid < 40$ cm where the mean position $\bar{z}$ of the nominal interaction point varies between ± 5 cm around $z = 0$ depending on the HERA beam settings. Moreover, events must fulfil an electron or large missing transverse momentum trigger requirement [18].

The selection criteria specific to each of the studied event topologies are presented below. These rely basically on the final state lepton finding and on global energy-momentum conservation cuts optimized separately for each case using Monte-Carlo simulation.

5.2 Event selection for topology S1

Squarks decaying via S1 are characterized by NC DIS-like signatures. The scattered positron is expected to have a high transverse energy $E_{T,e}$ due to the Jacobian peak at $M_{\tilde{q}}/2$ of the $E_{T,e}$ distribution. The squark mass is related to the usual Bjorken x via $M = \sqrt{xs}$. Squarks being scalar particles, they decay isotropically in their centre of mass (CM) frame. Hence, the usual DIS Bjorken scattering variable y, which is related to the positron polar angle θ_e^* in the $e - q$ CM frame via $y = (1 + \cos\theta_e^*)/2$ is uniformly distributed for such events. This contrasts with the steeply falling $1/y^2$ dependence expected for NC DIS at fixed mass (i.e. fixed x). Hence the strategy is to look for resonances in NC DIS-like events at high M and high y, i.e. at high Q^2. Selection requirements are thus similar to those described in [1] where observation of DIS events at very high Q^2 was reported. The complete set of selection cuts can be found in [16] where a search for leptoquarks in H1 is presented in detail.

The main selection criteria are the following :

1. an isolated positron with $E_{T,e} > 15$ GeV ($E_{T,e} = E_e \sin\theta_e$), found within the polar angular range $5^\circ \leq \theta_e \leq 145^\circ$;

2. a total transverse momentum balance $P_{T,miss}/\sqrt{E_{T,e}} \leq 4\sqrt{\text{GeV}}$ where $P_{T,miss} \equiv \sqrt{(\sum E_{x,i})^2 + (\sum E_{y,i})^2}$ summed over all energy deposits i in the calorimeters ($E_{x,i} = E_i \sin\theta_i \cos\phi_i$ and $E_{y,i} = E_i \sin\theta_i \sin\phi_i$);

3. a limited longitudinal momentum loss in the direction of the incident lepton, $40 \leq \sum (E - P_z) \leq 70$ GeV, where $\sum (E - P_z) \equiv \sum (E_i - E_{z,i})$ with $E_{z,i} = E_i \cos\theta_i$;

4. the usual DIS Lorentz invariant y should lie within the range $0.1 < y < 0.9$.

The identification of the scattered positron relies on the properties of electromagnetic showers [19, 23] and isolation criteria described in [9]. We use in the following the measurement of the scattered positron energy and angle to reconstruct the variables M, y and Q^2, henceforth labelled M_e, y_e and Q^2_e. Kinematic formulae can be found in [1, 16]. The cut (2) maintains a high selection efficiency for NC DIS-like events up to the highest $E_{T,e}$, by taking into account the natural scale of the hadronic energy resolution for e + jet events. Cut (3) provides a powerful rejection of photoproduction contamination and also suppresses NC DIS-like events with a very hard γ emitted from the initial state positron, by exploiting the fact that $\sum (E - P_z)$ should peak at $2E^0_e$ for events where only particles escaping in the proton direction remain undetected. Cut (4) avoids the low y region where the M_e resolution severely degrades. The cut $y_e < 0.9$ efficiently reduces the remaining γp contamination and avoids the domain where QED radiative effects can be important. The analysis is moreover restricted to $Q^2_e > 2500$ GeV^2.

The signal significance is then optimized by applying in addition a M_e dependent y_e cut [16]. This y_e cut varies from $y_e \gtrsim 0.6$ at 60 GeV to $y_e \gtrsim 0.4$ at 200 GeV and down to $y_e \gtrsim 0.2$ above 250 GeV. We observe 312 events satisfying all the above requirements in the mass range $M_e > 62.5$ GeV, which is in good agreement with the SM expectation of 306 ± 23 (the sources of systematic errors will be described in section 5.7). The measured mass spectrum of these candidates is compared to the NC DIS expectation in Fig. 2a. This figure also shows the important background reduction achieved when applying the optimized y_{cut} instead of the fixed cut $y_e > 0.1$. Data are found to be well described by Monte-Carlo, although an excess of events still remains for masses $M_0 \simeq 200$ GeV where 8 events are observed while 3.01 ± 0.54 are expected in the range $M_0 \pm \Delta M_0/2$ with $\Delta M_0 = 25$ GeV. This "clustering" is however less significant than that observed with $94 \to 96$ data alone [1].

In this channel, the $\not{R}_p$ SUSY signal detection efficiency is found to vary between 35% at 75 GeV, $\simeq 50\%$ at 200 GeV and 70% at 250 GeV.

5.3 Event Selection for topology S2

Squarks undergoing S2 decays lead to CC DIS-like signatures with high missing transverse momentum due to the high E_T escaping neutrino. In contrast to the S1 channel, only $\tilde{d}^{k*}_R$ squarks, produced via a fusion between the incident e^+ and a $\bar{u}^j$ quark from the proton, can undergo such a decay. HERA sensitivity with an e^+ incident beam is thus lowered in this channel since a high x sea quark must participate in the fusion. The same holds for leptoquarks undergoing charged current decays, at least in minimal models [12]. The analysis performed to search for such leptoquarks and described in [16] is also relevant to seek squarks decaying via S2. Hence only the main cuts and results are presented here.

The S2 selection mainly requires :

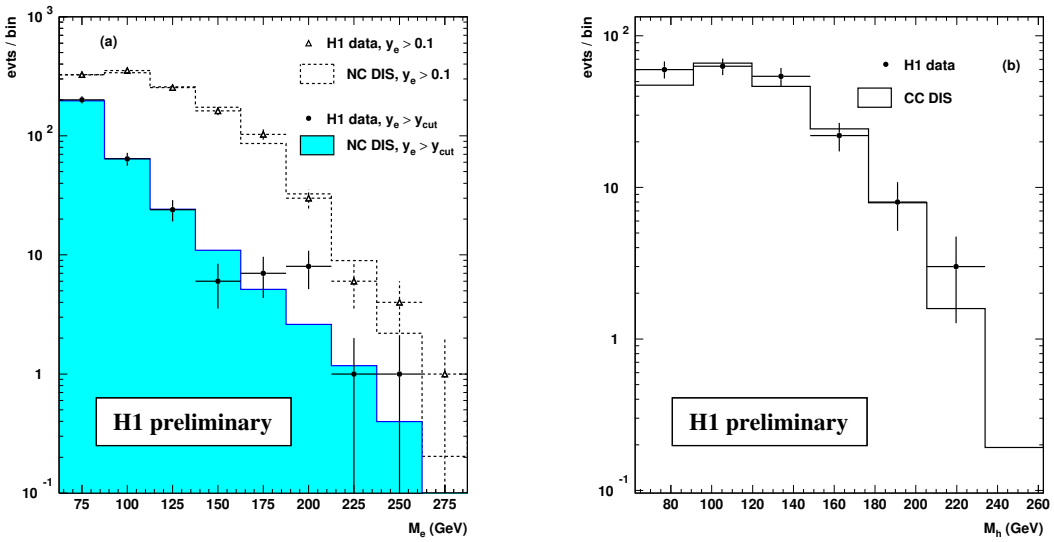

Figure 2: *Mass spectra for (a) $e + q$ (event topology S1) and (b) $\nu + q$ (event topology S2) final states for data (symbols) and NC DIS expectation (histogram).*

1. no $e^{\pm}$ candidate with $E_T > 5$ GeV found in the LAr calorimeter, using the same electron identification algorithm as used for S1;
2. a missing transverse momentum $P_{T,miss} > 30$ GeV;
3. that the Lorentz y variable reconstructed from the hadronic energy flow statisfy $y_h < 0.9$.

These cuts eliminate NC DIS and photoproduction backgrounds. The high y_h domain, where the resolution on the mass $M_h = \sqrt{x_h s}$ reconstructed from the hadronic energy flow becomes poor [1], is excluded from the analysis by cut (3). As for the S1 channel, we concentrate on the high Q^2 domain by requiring $Q^2_h > 2500$ GeV^2.

We observe 210 events satisfying these requirements in the mass range $M_h > 50$ GeV, which agrees well with the CC DIS expectation of 193.7 ± 28.5. The observed and expected mass spectra are shown to be in good agreement in Fig. 2b.

The $\not{R}_p$ SUSY signal detection efficiency in this channel, determined from Monte-Carlo, varies between $\simeq 27\%$ for a 75 GeV squark mass, to $\simeq 57\%$ at 100 GeV and $\simeq 78\%$ at 200 GeV. In the lowest mass range the efficiency is limited due to the high $P_{T,miss}$ requirement.

5.4 Event Selection for topology S3

For gauge decays of squarks leading to a "right" sign final state lepton (e.g. $e^+q' \to \tilde{q} \to \chi^0_1 + q \to e^+q''\bar{q}''q'$), we require :

1. one "positron" candidate in the angular range $5° < \theta_e < 110°$ with $E_{T,e} > 5$ GeV, using the same positron identification criteria as used for S1; one track has to be found within a

pseudorapidity-azimuth cone of radius $\sqrt{\Delta\eta^2 + \Delta\phi^2} = 0.25$ centered on the e candidate; this track must be made of at least 20 digitisations in the central and/or forward tracking system(s); moreover, the impact point of this track at the inner surface of the LAr must be at least 2° in azimuth away from each of the eight ϕ cracks separating octants of the LAr calorimeter;

2. that the y variable reconstructed using the energy and polar angle of the scattered e should satisfy $0.4 < y_e < 0.95$;

3. a total transverse momemtum balance $P_{T,miss} < 20$ GeV and a limited momentum loss in the direction of the incident lepton $40 \leq \sum (E - P_z) \leq 70$ GeV;

4. there is at most a small amount of energy deposited in the backward calorimeters, $E_{back} < 7.5$ GeV;

5. no energy E_{e-tag} in the e-tagger, unless $\mid E_{e-tag} + E_{\gamma-tag} - E_e^0 \mid < 5$ GeV, where $E_{\gamma-tag}$ is the energy in the γ-tagger, in order to save events which coincide randomly with Bethe-Heitler bremsstrahlung;

6. at least two jets in the angular range $7^\circ < \theta < 145^\circ$ and with $E_T > 7$ GeV; these are found using a cone algorithm in the laboratory frame with a radius $\sqrt{\Delta\eta^2 + \Delta\phi^2} = 1$; the fraction of the jet energy deposited in the electromagnetic part of the calorimeter must be below 5%; moreover, the highest P_T jet is required to satisfy $\theta > 10^\circ$ and $E_T > 15$ GeV;

7. that the jet among the two highest P_T jets selected as explained above, for which the polar angle $\theta_{backward}$ is maximal, verifies :

$$y_e - 0.4 > (\theta_{backward} - 25^\circ) \times (0.9 - 0.4)/(145 - 25)$$

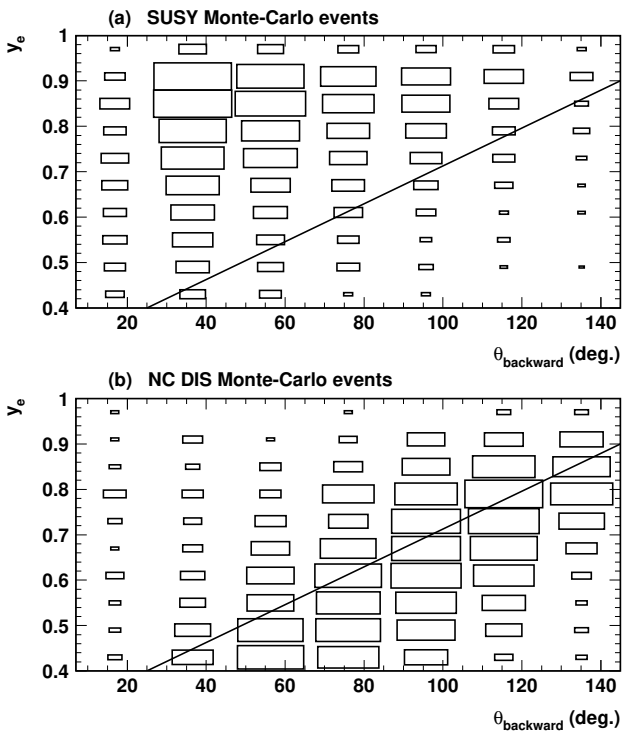

Figure 3: *Correlation between the y_e variable reconstructed from the e measurement and the angle $\theta_{backward}$ of the most backward jet for (a) SUSY Monte-Carlo events in which the squark decays via S3 and (b) NC DIS Monte-Carlo events, when all S3 selection cuts but cut (7) are applied. Cut (7) only retains events above the drawn full line.*

In events with the S3 topology, the scattered e arises from the decay of the last χ appearing in the decay chain and it only takes away a fraction of the momentum of this χ. Hence its energy can be quite small and the cut applied on $E_{T,e}$ is lower than that used in the S1 analysis, in order to maintain a high enough efficiency for the searched signal. The enhancement of γp contamination induced by the loosening of $E_{T,e}$ cut is compensated by the more stringent criteria applied to the e candidate which are described in cut (1). Moreover, for squarks decaying via S3, the final state e is strongly boosted in the direction of the incident proton, such that the $\theta_e < 110^\circ$ requirement discriminates powerfully the signal from NC DIS background. Cut (2), by selecting high y_e events, strongly suppresses NC DIS background while retaining high efficiency for the signal. Indeed, the $y_e = 1 - E_e/E_e^0 \sin^2(\theta_e/2)$ distribution reconstructed from the measurement of the scattered e appears strongly shifted towards large y_e in SUSY events for the reasons given above. Photoproduction background is efficiently suppressed by the cluster-track link and $y_e < 0.95$ requirements. Cut (4) reduces low Q^2 NC DIS and γp background, the latter being further suppressed by cut (5). Cut (6) ensures enough hadronic activity and a multijet topology. Since squark decays lead to events with high total transverse energy, we require at least one "hard" jet, far enough from the proton remnant to ensure a reliable measurement of its energy. Cut (7) exploits the fact that, for high y_e NC DIS events satisfying the above set of cuts, one hard jet is usually scattered in the backward region of the calorimeter. On the contrary, jets coming from a squark decaying via S3 will be boosted in the forward direction, independently of y_e. The effect of this cut and how it separates the signal from the remaining NC DIS background is illustrated in Fig. 3. In Fig. 3a, several sets of $(M_{\tilde{q}}, M_{\tilde{\chi}})$ are combined. The effect of cut (7) on signal events depends on these masses but retains a high efficiency over the whole range considered here.

We find 289 candidates satisfying the above set of cuts, which is in good agreement with the mean SM background of 285.7 ± 28.0 expected from NC DIS and photoproduction (γp processes contribute to less than 3%). Fig. 4 shows, for these candidates, the distributions of the Lorentz invariant y_e, the polar angles $\theta_{forward}$, $\theta_{backward}$ of the most forward and most backward jets among the two highest P_T jets, and the transverse momentum $P_{T,forward}$ of the forward jet. For all these variables, the data are well described both in shape and in normalization by the SM expectation.

An invariant mass M_{inv} is then calculated using the energy $E_{wrm} = \sum_i E_i$ where the sum runs over all energy deposits in the calorimeters at $\theta > 10^\circ$ in order to exclude the proton remnant. Ideally the squark mass should be equal to $\sqrt{4xE_e^0E_{wrm}}$. Bad measurements of the hadronic flow can alter this relation, and the variable $\sum(E - P_z)$ is used to estimate the induced under- or over-estimation of the squark mass, which is thus reconstructed as :

$$M_{inv} = \sqrt{4xE_e^0E_{wrm}} - \frac{\sum(E - P_z) - 2E_e^0}{2}$$

This reconstruction method improves the peak mass resolution for squarks decaying via S3 by a factor $\simeq 2$ compared to H1 previous published analysis [10], this resolution being typically 7 GeV for a 200 GeV squark mass.

The measured mass spectrum of the S3 selected events is compared to SM expectation in Fig. 5a good agreement is observed. The previous analysis [10] using only 1994 e^+p data showed a slight excess (2.9σ) in the invariant mass spectrum for masses around 80 GeV. This is clearly not confirmed with the additional statistics analysed here. In Fig 5a, a small excess of events is observed at the highest masses but this is not very significant taking into account the total error on the SM expectation, as can be seen in Fig. 5b where the lines above and below

unity specify the $\pm 1\sigma$ error band determined using the combination of statistical and systematic errors.

In this channel, the $R\!\!\!/_p$ SUSY signal detection efficiencies (which experimentally sums that of both the $right\ sign$ and the $unsigned$ events), depend mainly on the mass of the χ entering the decay chain. Typical values are $\simeq 50\%$ for a 200 GeV squark decaying into a 80 GeV χ_1^0, and $\simeq 36\%$ when these masses are set respectively to 100 GeV and 40 GeV.

5.5 Event Selection for topology S4

For a gauge decay of the squarks leading to a "wrong" sign final state lepton (i.e. $e^+q' \to \tilde{q} \to e^-q''\bar{q}''q'$) we apply the same requirements as for channel S3 and perform a determination of the lepton charge using the tracking chamber information.

In addition to the S3 selection cuts, we require that there be only one track found in the e isolation cone. This track is required to correspond to a negatively charged particle and must moreover satisfy the following criteria :

1. the track momentum P must match the calorimetric energy E_e of the e candidate within : $P/E_e > 0.5$;
2. the error on the track curvature κ must verify $\mid \kappa/\delta\kappa \mid > 2$.

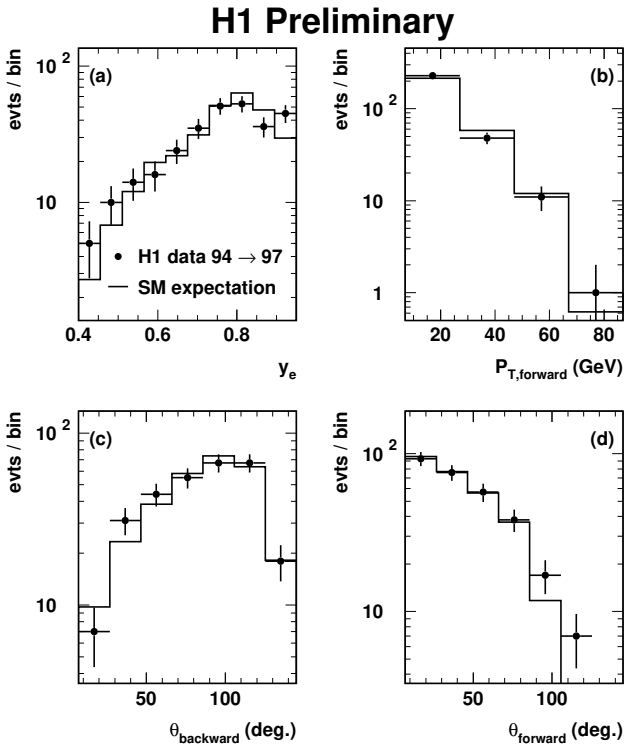

Figure 4: *For S3 candidates, distributions of (a) y_e, (b) the transverse momentum $P_{T,forward}$ of the most forward jet, (c) the polar angle $\theta_{backward}$ of the most backward and (d) $\theta_{forward}$ of the most forward jet.*

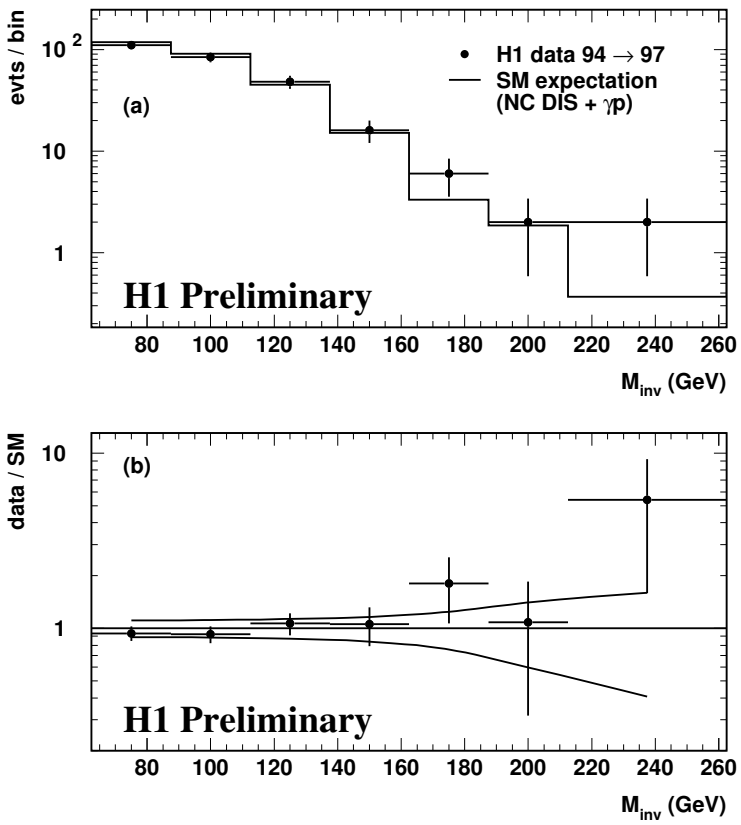

Figure 5: *(a) Mass spectrum for e + multijets final states (event topology S3) for data (symbols) and NC DIS expectation (histogram); (b) ratio of the observed and expected number of events as a function of M_{inv}; the lines above and below unity specify the $\pm 1\sigma$ levels determined using the combination of statistical and systematic errors of the NC DIS expectation.*

These cuts ensure a good quality of the track reconstruction at the expense of a reduced efficiency. We found that the fraction of S3 selected candidates which fulfil these additional requirements is $\simeq 62\%$. This is well reproduced by the NC DIS simulation, which predicts an efficiency loss of $\simeq 34\%$ in the phase space relevant for S3 analysis. We thus rely on the SUSY Monte-Carlo to estimate the efficiency loss ε_{loss} of above cuts (1) and (2) on the signal as a function of the squark mass. The difference of 4% on the determination of ε_{loss} obtained when using data or NC DIS Monte-Carlo events reflects the level at which the tracking performance is described by the simulation, and will be taken as a systematic error on ε_{loss}.

One such wrong sign candidate is observed in the data, while the SM prediction as estimated from Monte-Carlo is 0.49 ± 0.2 (coming from NC DIS).

5.6 Event Selection for τ + jet final states

We now consider the case where two $\not{R}_p$ couplings λ'_{1jk} and λ'_{3jl} are non-vanishing and dominate over the remaining $\not{R}_p$ Yukawa couplings. Under these conditions, squarks could be produced via the λ'_{1jk} coupling and decay via λ'_{3jl}, leading to one high P_T τ lepton and a high P_T jet. In

[16] a search for leptoquarks possessing couplings to both $e - q$ and $\tau - q'$ pairs is reported. The signal in the τ + jet channel is sought considering the hadronic decays of the τ lepton. The same analysis is performed here, hence only the main requirements are reminded.

Inclusive τ + jet signatures, where the τ lepton decays into hadrons, are selected by requiring :

1. two jets found in the angular range $7^\circ < \theta < 145^\circ$ using the cone algorithm described above, with transverse momentum $P_T > 30$ GeV;
2. one of these must be a "pencil-like" jet, i.e. with small invariant mass $M_{jet} < 7$ GeV and a low track multiplicity $1 \leq N_{tracks} \leq 3$, N_{tracks} being the number of vertex fitted tracks with $P_T > 0.15$ GeV in the jet isolation cone;
3. the leading track of the τ-jet candidate (i.e. the track with the highest fraction of the τ-jet calorimetric energy E_{jet}) is required to carry at least 10% of E_{jet};
4. the energy E_{track} of this leading track must verify : $E_{track}/E_{jet} + f_{em} < 1.5$, where f_{em} is the electromagnetic fraction of the τ-jet candidate.

Cut (3) efficiently reduces γp background where a low multiplicity jet fakes a τ-jet. Cut (4) suppresses NC DIS background where the scattered positron has not been identified. It exploits the fact that the electromagnetic fraction of a τ-jet is high mainly when the τ lepton decays to $n\pi^0 + X$, which leads to a small value for the ratio E_{track}/E_{jet}. On the contrary, for NC DIS events where e.g. the positron has been lost in a crack in the calorimeter, this ratio is expected to peak at one.

We observe 28 events satisfying the above inclusive τ + jet requirements, which agrees well with the mean expectation of 23.7 ± 5.7 events coming from NC DIS and γp processes.

Additional cuts relevant for the specific process $\tilde{q} \to \tau +$ jet are then applied :

1. the missing transverse momentum $P_{T,miss} > 10$ GeV ;
2. the total hadronic final state and the τ jet candidate must be back-to-back in the plane transverse to the beam axis : $\Delta\phi_{\tau-h} > 165^\circ$.

Both these cuts exploit the fact that neutrino(s) emerging from the τ decay are collimated with the τ jet direction, and that the other jet in $\tilde{q} \to \tau +$ jet events is formed by the fragmentation of a quark and thus should not contribute to the missing transverse momentum.

None of the 28 above selected events fulfil these last requirements, while 0.8 ± 0.3 events are expected from SM processes.

This selection ensures an efficiency which ranges from $\simeq 10\%$ for a 100 GeV squark decaying into $\tau +$ jet to $\simeq 25\%$ for squark masses above 200 GeV.

5.7 Systematic Errors

In each channel analysed in the previous sections, the error on the mean expectation from Standard Model processes has been calculated by taking into account the systematic errors described below.
The experimental error sources considered are the following :

- the uncertainty of $\pm 2.3\%$ on the integrated luminosity which affects equally the SM expectations for each channel;
- the uncertainty on the absolute calibration of the calorimeters for electromagnetic energies, ranging between $\pm 1\%$ in the central wheels and $\pm 3\%$ in the forward region of the LAr calorimeter; this constitutes the main error source for the estimation of NC DIS background to channel S1;
- the uncertainty of $\pm 4\%$ on the absolute hadronic energy scale. This contributes for channel S3 and is the main error source for channel S2 and for the SM expectation in the τ + jet analysis.

The estimates of SM expectations also suffer from theoretical uncertainties which are summarized below :

- for channel S1 (NC DIS-like final states), the uncertainty of $\pm 5\%$ on parton density distributions obtained by QCD fits; for CC DIS-like topologies (channel S2), which are mainly induced by d quarks whose density in the proton is less constrained, this uncertainty increases linearly with Q^2 up to $\simeq 20\%$ at the highest Q^2 considered here;
- the value of the strong coupling constant α_S, leading to an uncertainty of $\pm 4\%$;
- for channels S1, S3 and S4, higher order QED corrections imply a $\pm 2\%$ uncertainty in the y range considered here.

All the analyses have been repeated with a shift of the central value of each of the sources of errors by ± 1 standard deviation to estimate their individual contribution. The overall systematic error on SM expectations is then determined as the quadratic sum of the resulting errors and of the statistical error on the Monte-Carlo simulation.

6 Results

Apart from an excess at $M_e \sim 200$ GeV in channel S1, no significant deviation from the SM expectations has been found in the various $\not{R}_p$ and gauge decay channels analysed in section 5. Assuming that the observed excess of events in the NC DIS-like channel is due to a statistical fluctuation (or, formally, that the observation contains at most two components, an unknown "resonance" signal and a known expectation from NC DIS), the various decay channels can be used and combined to set constraints on $\not{R}_p$ SUSY models.

As mentioned in section 2, when HERA operates with an incident beam of positrons, the best probed $\not{R}_p$ couplings are λ'_{1j1} which allow for resonant production of $\tilde{u}^j_L$ squarks. Hence

we concentrate here on these λ'_{1j1} couplings, assuming one of them is non-vanishing for a given index j. In this section, mass dependent upper rejection limits on the Yukawa couplings λ'_{1j1} are first derived using, for each contributing channel, the branching ratios, the signal detection efficiencies and the numbers of observed and expected events. Models with two non-vanishing couplings λ'_{1j1} and λ'_{3jk} are also constrained in section 6.2.

6.1 Rejection limits on λ'_{1j1}

We assume here that one of the λ'_{1j1} is non-vanishing and derive rejection limits on this coupling as a function of the $\tilde{u}^j_L$ mass, combining all contributing channels. The masses of sparticles other than $\tilde{u}^j_L$ only influence slightly the branching ratios of the neutralinos and charginos [11]. Hence results presented here weakly depend on the masses of other sparticles and no degeneracy assumption needs to be made. As already mentioned before, gauge invariance forbids the $\tilde{u}^j_L$ to decay into $\nu + q$ and thus the only relevant channels are S1, S3 and S4.

Mass dependent upper limits on the production cross section $\sigma(e^+ + p \to \tilde{u}^j_L)$ are obtained assuming Poisson distributions for the SM background expectations and for the signal. Each channel Sk contributes in the limits derivation via its total branching ratio β_k, the numbers of observed and expected events satisfying Sk selection cuts, and the corresponding selection efficiency. For channels S1 and S3, the numbers of observed and expected events are integrated within a mass bin which slides over the accessible mass range. The width of the mass bin is adapted to the expected mass resolution in each channel, so that this bin contains approximately 68% of the signal at a given squark mass. For example, the mass bins used to constrain a 200 GeV squark are $[186; 204]$ GeV and $[189; 206]$ GeV for S1 and S3 channels respectively. For channel S4 where both the expectation and the observation are small, no mass restriction is imposed.
Both systematic and statistical errors have been folded in channel by channel as described in [9]. In addition to the systematic errors on the SM expectations described in the previous section, the following uncertainties have been considered in the derivation of rejection limits :

- the lack of knowledge of the d quark density in the proton leads to an uncertainty on the $e^+ + d \to \tilde{u}^j_L$ cross section, which varies between $\simeq 5\%$ at low masses and $\simeq 20\%$ around 250 GeV;
- choosing Q^2_e, or $P^2_{T,e}$ instead of $M^2_{\tilde{q}}$ as the hard scale at which the parton distributions are estimated induces an uncertainty of $\pm 7\%$ on the cross section $e^+ + d \to \tilde{u}^j_L \to e^+ + d$, and thus on the squark production cross section;
- for channel S1, the effect of the interference between standard NC DIS and the $e^+ + d \to \tilde{u}^j_L \to e^+ + d$ process has been studied and was found to be negligible.

The masses of the neutralinos and charginos, as well as the gauge couplings between any two SUSY particles and a standard fermion/boson, are determined by the usual MSSM parameters : the "mass" term μ which mixes the Higgs superfields, the soft-breaking parameter M_2 for $SU(2)$ gauginos and the ratio $\tan\beta$ of the vacuum expectation values of the two neutral scalar Higgses. For a fixed set of these MSSM parameters and a given squark mass, the branchings β_k in the different channels Sk only depend on λ'_{1j1}. This also holds for the upper limit on the cross section $\sigma_{\tilde{u}^j_L}(\lambda')$ derived from the combination of the analysed channels. The upper limit on λ'_{1j1} at a given squark mass is then obtained by solving iteratively the equation :

$\sigma_{\tilde{u}_L^j}(\lambda') = \sigma(e^+p \to \tilde{u}_L^j)$ where the production cross section $\sigma(e^+p \to \tilde{u}_L^j)$ approximately scales with λ'^2_{1j1}.

Cascade decays involving any chargino or neutralino can in principle contribute to channels S3 and S4 (an example of a cascade decay chain involving the χ_1^+ and leading to S3 final state is given in table 2). Such decay chains involving the heaviest χs would lead to final states with very high jet multiplicities, for which the calculations of signal efficiencies are not straightforward. Hence, only cascades involving the lightest chargino χ_1^+ and the second lightest neutralino χ_2^0 are taken into account in the calculation of branching ratios into S3 and S4, though squark decays into heavier χ states are allowed and contribute to the total squark width. As an example, the total branching in channel S3 is determined as follows :

$$\begin{aligned}\beta_3 &= \beta(\tilde{u}_L^j \to q\chi_1^0) \times \beta_1^0 + \beta(\tilde{u}_L^j \to q\chi_2^0) \times \beta_2^0 + \beta(\tilde{u}_L^j \to q\chi_1^+) \times \beta_1^+ \\ &+ \beta(\tilde{u}_L^j \to q\chi_2^0) \times \beta(\chi_2^0 \to \chi_1^0 q\bar{q}) \times \beta_1^0 + \beta(\tilde{u}_L^j \to q\chi_1^+) \times \beta(\chi_1^+ \to \chi_1^0 qq') \times \beta_1^0\end{aligned}$$

where β_i^0 and β_j^+ represent the branching of χ_i^0 and χ_j^+ decaying via $\not{R}_p$ into $e^+ + 2$ jets. This determination is conservative, and it can be checked that, in the mass range considered here, squark decays into $\chi_{1,2}^0$ and χ_1^+ already represent a high fraction of the total squark gauge decays.
The relevant decay widths of all involved sparticles have been obtained using the SUSYGEN package [35], and taking into account all possible $\not{R}_p$ and gauge decays.

Rejection limits obtained at the 95% confidence level (CL) on λ'_{1j1} as a function of the $\tilde{u}_L^j$ mass are shown in Fig. 6a where the channels taken into account are S1 only (solid line), S1 and S3 (dashed line), or all contributing channels S1, S3 and S4 (dotted line). Domains above the curves are excluded. The MSSM parameters have here been set to $\mu = -200$ GeV, $M_2 = 70$ GeV and $\tan\beta = 1.5$. With this choice of parameters, the lightest neutralino χ_1^0 is mainly dominated by its photino component and its mass is about 40 GeV, while the χ_1^+ and χ_2^0 are nearly degenerate around 90 GeV. Combining the three contributing channels improves the sensitivity considerably, up to a factor $\simeq 5$ at lowest masses, compared to what is achived using only the $e + q$ data (i.e. channel S1). The relative contributions of channels S1, S3 and S4 are shown in Fig. 6b against the squark mass, at the current sensivity limit on the Yukawa coupling. For masses up to $\simeq 230$ GeV, channels S3 and S4 have similar dominant contributions. As soon as squark decays into χ_1^+ and χ_2^0 become kinematically allowed, β_3 and β_4 are hampered by the fact that both χ_1^+ and χ_2^0 decay preferentially into $\nu q\bar{q}$ instead of $e^{\pm}qq'$ (because they are dominated respectively by their wino and zino components [10, 13, 14, 15]). In the very high mass domain, a large Yukawa coupling is necessary to allow squark production, hence the relative contribution of S1 is largely enhanced.

In order to study the dependence of our rejection limits on the MSSM parameters, another set of values for $(\mu, M_2, \tan\beta)$ leading to a 40 GeV χ_1^0 dominated by its zino component is chosen. The masses of χ_1^+ and χ_2^0 are then respectively $\simeq 100$ GeV and $\simeq 72$ GeV. As before, 95% CL limits on λ'_{1j1} versus the squark mass are displayed in Fig. 6c. The gain obtained by the combination of the three channels is less substantial than in the previous case. Indeed the χ_1^0, dominated here by its $\tilde{Z}$ component, decays with a high branching ratio into $\nu q\bar{q}$ instead of $e^{\pm}qq'$. The same holds for the lightest chargino. Hence, total branchings β_3 and β_4 are quite small though gauge decays of the squark are important. In contrast with the "photino" case, β_3 is here substantially higher than β_4. This is mainly due to the fact that the fraction of $\not{R}_p$ decays into $\nu q\bar{q}$ is smaller for the χ_1^+ than for the χ_1^0. In fact, the dominant decay channel here is the one labelled S5 in [10], leading to multijets + $P_{T,miss}$ topology, which has not been addressed

in this paper. The separation of the signal from the SM background in this channel is however not easy, and, following the analysis presented in [10], we expect that the limit obtained when also combining S5 would not improve too much the result given here.

Since the gauge decay width of the squark does not depend on the Yukawa coupling λ'_{1j1}, the regions of the plane $(\beta_1, M_{\tilde{q}})$ above the dotted lines in Fig. 6b and Fig. 6d are excluded at 95% CL by our combined analysis. In particular the branching ratio of a 200 GeV $\tilde{u}^j_L$ squark into $e^+ + q$ is constrained to be smaller than $\simeq 1.5\%$ (Fig. 6b) or $\simeq 6\%$ (Fig. 6d) for the two choices of MSSM parameters presented here. It should be noted however that other choices of $(M_2, \mu, \tan\beta)$ allow a 200 GeV squark to decay via S1 with a branching ratio above 10%.

Limits obtained when combining S1, S3 and S4 for the two cases detailed above are compared to each other in Fig. 7. Our sensitivity on λ'_{1j1} for squark masses below $\simeq 200$ GeV is better by a factor $\simeq 2$ for a $\tilde{\gamma}$-like χ^0_1 than for a χ^0_1 dominated by its zino component, due to the higher part of total branching actually being "seen" by our analysis. One can infer from [10] that the two cases presented here are somewhat "extreme" and in that sense quite representative of the sensitivity we can achieve for any other choice of MSSM parameters leading to a 40 GeV χ^0_1. The same figure shows the 95% CL limits obtained for a 100 GeV and a 150 GeV $\tilde{\gamma}$-like χ^0_1. The sensitivity achieved increases with the $\tilde{\gamma}$ mass due to the higher efficiencies in channel S3. For electromagnetic coupling strengths $\lambda'^2_{1j1}/4\pi \simeq \alpha_{em}$ (i.e. $\lambda'_{1j1} \simeq 0.3$), squark masses up

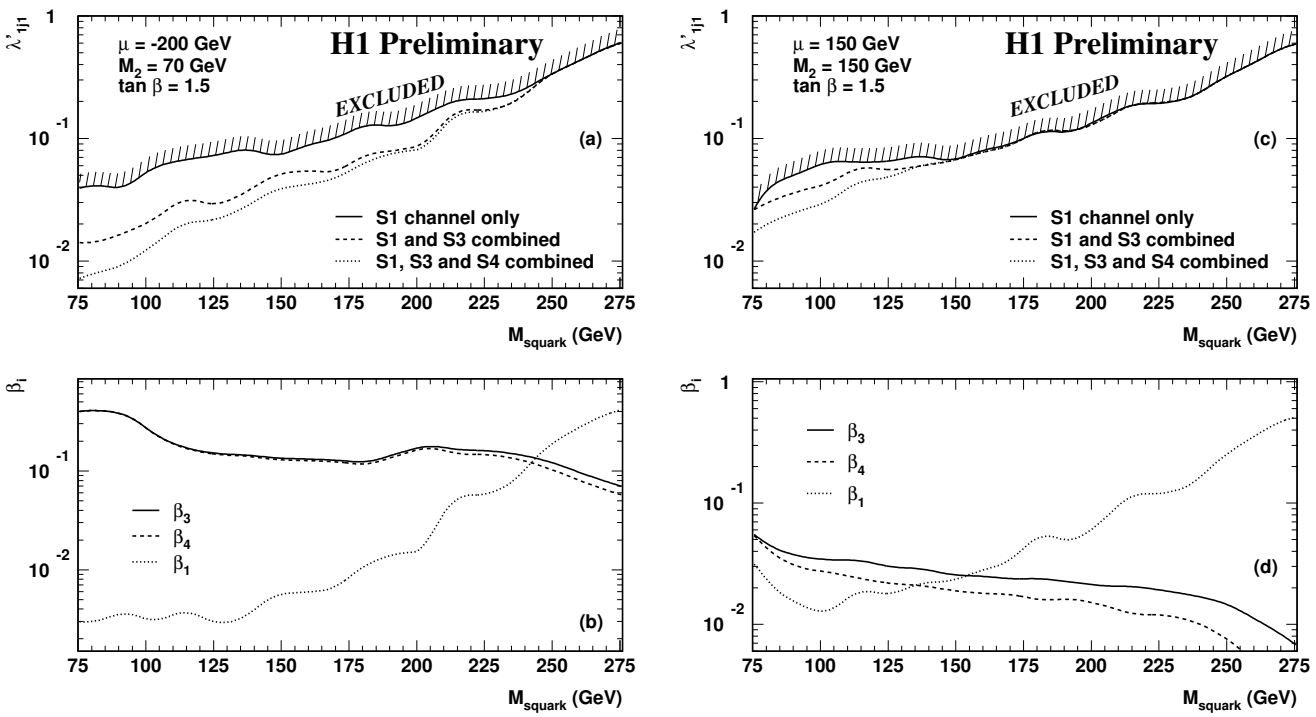

Figure 6: *(a) Exclusion upper limits at 95% CL for the coupling λ'_{1j1} as a function of the squark mass, for a set of MSSM parameters leading to a 40 GeV χ^0_1 dominated by its photino component. The limits are given with different combinations of the contributing channels. Regions above the curves are excluded; (b) The relative contributions of channels S1, S3 and S4 versus the squark mass; (c) and (d) : as (a) and (b) but for a 40 GeV χ^0_1 dominated by its zino component.*

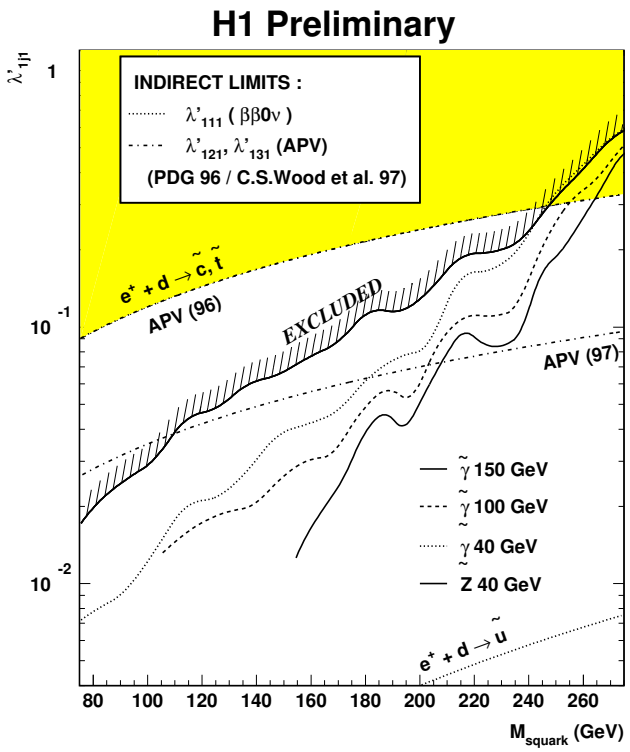

Figure 7: *Exclusion upper limits at* 95% *CL for the coupling* λ'_{1j1} *as a function of squark mass, for various masses and mixtures of the* χ^0_1*; also represented are the most stringent indirect limits on* λ'_{111} *and* λ'_{1j1}, $j = 2, 3$.

to 262 GeV are excluded at 95% CL by this analysis, and up to 175 GeV for coupling strengths $\simeq 0.01\alpha_{em}$. For low masses, these limits represent an improvement of a factor $\simeq 3$ compared to previously published H1 results [10].

Relevant searches for scalar leptoquarks have been performed by both the $D\emptyset$ [6] and CDF [7] experiments at the TeVatron collider. These rule out $\tilde{u}^j_L$ squark masses below 200 GeV as soon as the branching ratio of the squark into $e^+ + q$ is greater than $\simeq 50\%$, but the excluded mass domain does not extend above $\simeq 110$ GeV for values of this branching below 10%. Since in $\not{R}_p$ SUSY such a branching can be naturally small, as can be seen in Fig. 6b and d, such leptoquark-like constraints are easily evaded.

Specific SUSY searches have also been carried out at the TeVatron collider, mainly in the Minimal Supergravity (mSUGRA) frame (imposing mass relations between the sparticles) and assuming R-parity conservation. Recently the $D\emptyset$ experiment [36] also studied the pair production of squarks in $\not{R}_p$ mSUGRA, looking at like-sign dielectron events accompanied with jets. Squark masses below 252 GeV are ruled out by this analysis assuming five degenerate squarks. A similar analysis considering models in which R-parity is violated by λ'_{121} has been carried out by the CDF experiment [37], from which we infer that a five times smaller cross section would lead to a squark mass limit of $\simeq 150$ GeV, depending on the gluino and neutralino masses. Within the same model, the CDF experiment [37] also considered separately the pair production of a light stop $\tilde{t}_1$ and excluded stop masses below $\simeq 130$ GeV assuming that the stops decay into $c\chi^0_1$. If R-parity is violated by a λ'_{13k} coupling the $\not{R}_p$ decays of the stops would dominate over loop decays into $c\chi^0_1$, but be negligible compared to decays into $b\chi^+_1$ if

this latter mode is allowed (which implies $M(\tilde{t}_1) > M(\chi_1^+)$ and that there is a non-vanishing "left" component for the $\tilde{t}_1$ eigenstate). The subsequent decays of the χ_1^+ would then lead to final states similar to those studied by CDF in [37]. Thus we conclude that $130 - 150$ GeV is a reliable estimate of the TeVatron sensitivity on the light stop mass also in models in which R-parity is violated by a λ'_{13k} coupling.

Hence TeVatron and HERA sensitivities are competitive in $\not{R}_p$ SUSY models with five degenerate squarks, but models predicting a light stop are probably better constrained at HERA provided that the $\not{R}_p$ coupling λ'_{13j} is not too small.

Our results are also compared in Fig. 7 to the best indirect limits. The most stringent constraint comes from the non-observation of neutrinoless double beta decay [38] but only concerns λ'_{111} coupling. The most severe indirect limits on couplings λ'_{121} and λ'_{131}, which could allow for the production of squarks $\tilde{c}$ and $\tilde{t}$ respectively, come from Atomic Parity Violation [39]. Two constraints are given on the figure [40, 41] which depend on the experimental input [42, 43]. H1 direct limits are thus better or comparable to the most stringent constraints on λ'_{121}, λ'_{131}. For high χ_1^0 masses our limit even improves these indirect contraints by a factor up to $\simeq 4$.

6.2 Rejection limits on $\lambda'_{1j1} \times \lambda'_{3jk}$

Turning now to the case where two couplings λ'_{1j1} and λ'_{3jk} are non-vanishing, the analysis of τ + jet final states presented in the previous section is used to set constraints on the lepton flavor violating process $e^+ + p \to \tilde{u}_L^j \to \tau^+ + d^k$. In contrast to section 6.1, we assume here that the gauge decays of squarks are forbidden, so that the only squark decay modes are $\tilde{u}_L^j \to e^+ + d$ and $\tilde{u}_L^j \to \tau^+ + d^k$. Assuming a given value for the production coupling λ'_{1j1}, exclusion limits at 95% CL on λ'_{3jk} are derived. Results are shown in Fig. 8 against the $\tilde{u}_L^j$ mass, for λ'_{1j1} equal to 0.3 (i.e. an electromagnetic coupling strength), 0.1 and 0.03. Shaded domains are excluded. For $\lambda'_{1j1} = \lambda'_{3jk} = 0.03$, $\tilde{u}_L^j$ squarks lighter than 165 GeV are excluded at 95% CL. Relevant lepton flavour violation analysis have been carried out by the H1 [44] and ZEUS [45] experiments. A similar analysis to that presented here has been published by the ZEUS Collaboration, with an integrated luminosity of $\simeq 3$ pb^{-1} using e^+p 1994 data [45]. Instead of fixing λ'_{1j1}, results were presented assuming $\lambda'_{1j1} = \lambda'_{3jk}$. When these two couplings are both equal to 0.03, the analysis presented here extends the squark mass range excluded in [45] by $\simeq 65$ GeV.

Relevant searches for third generation leptoquarks have also been carried out by CDF [46] (looking at $\tau\tau bb$ final states) and $D\emptyset$ [47] (looking at $\nu\nu bb$ final states) experiments. Masses up to only $\simeq 99$ GeV were excluded by these analysis using the full available luminosity of $\simeq 110$ pb^{-1}.

The only relevant indirect limits [48] come from the processes $\tau \to \pi e$, $\tau \to Ke$ and $B \to \tau e X$, which respectively constrain the products $\lambda'_{1j1} \times \lambda'_{3jk}$ with $k = 1, 2, 3$. These indirect limits are indicated in Fig. 8 for $\lambda'_{1j1} = 0.3$ as the full, dashed and dotted lines. H1 direct limits improve these contraints by typically one order of magnitude. Note that better indirect limits on couplings λ'_{3jk} alone exist [41, 48], coming e.g. from $\tau \to \pi\nu$, $Z \to \tau\tau$, $K^+ \to \pi^+\nu\bar{\nu}$, or from $D^0 - \bar{D}^0$ mixing. However these only concern the $\tilde{d}_R^k$ and can thus be evaded assuming e.g. $\tilde{u}_L^j$ to be much lighter than other squarks, which could be achieved especially in the case $(j = 3)$ of a light stop.

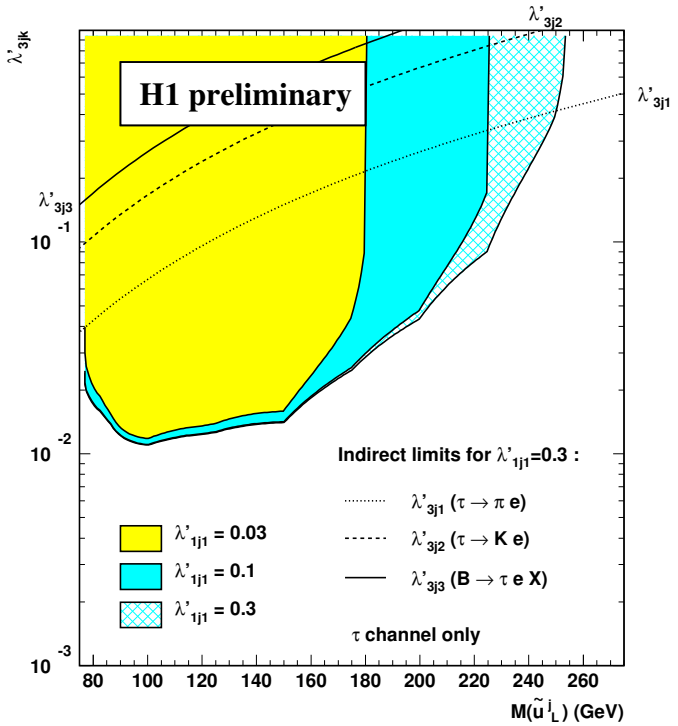

Figure 8: *Exclusion upper limits at* 95% *CL for the coupling* λ'_{3jk} *as a function of squark mass, for for several fixed values of* λ'_{1j1} *(greyed domains). The regions above the full, dashed and dash-dotted curves correspond to the best relevant indirect limits.*

7 Conclusions

We have searched for resonant squarks in ep collisions at HERA in R-parity violating as well as gauge decay modes. Notwithstanding an excess at $M_e \sim 200$ GeV in channel S1, no significant evidence for the production of squarks was found and mass dependent limits on the R-parity violating couplings were derived. The existence of squarks coupling to a e^+d pair with masses up to 175 GeV $(262$ GeV$)$ is excluded at 95% confidence level for a strength of the Yukawa coupling equal to $0.01 \times \alpha_{em}$ (α_{em}). Our limits extend beyond the domain covered by other colliders experiments, and, for some R-parity violating couplings, are better than the most stringent indirect constraints. No candidate for up-like squarks coupling to both eq and $\tau q'$ pairs has been observed and constraints on the Yukawa coupling involving the τ lepton have been set which extend far beyond previous relevant limits.

Acknowledgements

We wish to thank the HERA machine group as well as the H1 engineers and technicians who constructed and maintained the detector for their outstanding efforts. We thank the funding agencies for their financial support. We wish to thank the DESY directorate for the support and hospitality extended to the non-DESY members of the collaboration.

References

[1] H1 Collaboration, C. Adloff *et al.*, Z. Phys. C74 (1997) 191.

[2] ZEUS Collaboration, J. Breitweg *et al.*, Z. Phys.C74 (1997) 207.

[3] M. Drees, Phys. Lett. B403 (1997) 353.

[4] U. Bassler and G. Bernardi, Z. Phys. C76 (1997) 223.

[5] D. Choudhury and S. Raychaudhuri, Phys. Lett. B401 (1997) 54; G. Altarelli *et al.*, Nucl. Phys. B506 (1997) 3; H. Dreiner and P. Morawitz, Nucl. Phys. B503 (1997) 55; T. Kon and T. Kobayashi, Phys. Lett. B409 (1997) 265; G. Altarelli, G.F. Giudice and M.L. Mangano, Nucl. Phys. B506 (1997) 29; J. Ellis, S. Lola, K. Sridhar, Phys. Lett. B408 (1997) 252; J.E. Kim and P. Ko, Phys. Rev. D57 (1998) 489; S. Lola, Proceed. of the 5th Int. Workshop on Deep Inelastic Scattering and QCD, Chicago, USA, (April 14-18, 1997) 5pp.; G. Altarelli, Proceedings of the SUSY 1997 Conference, Nucl. Phys. Proc, Suppl. 62 (1998) 3; R. Rückl, H. Spiesberger, Proceed. of the Workshop New Trends in HERA Physics, Tegernsee, Germany (May 25-30,1997) 14pp.; A. S. Joshipura, V. Ravindran and S. K. Vempati, Phys. Rev. D57 (1998) 5327; J. Ellis, Proceed. of the Europhysics Conf. on High-Energy Physics, Jerusalem (August 1997) 8pp.; S. Raychaudhuri, Proceed. of the Int. Workshop on Physics Beyond the Standard Model, Valencia, Spain (October 13 - 17, 1997) 5pp.; E. Asakawa, J. Kamoshita and A. Sugamoto, Ochanumizu Univ. preprint PP-115 (March 1998) 15pp..

[6] D$\emptyset$ Collaboration, B. Abbott *et al.*, Phys. Rev. Lett. 79 (1997) 4321;
idem, Phys. Rev. Lett. 80 (1998) 2051.

[7] CDF Collaboration, F. Abe *et al.*, Phys. Rev. Lett. 79 (1997) 4327.

[8] see http://www-d0.fnal.gov/public/new/analyses/lq/lq_mar98.html

[9] H1 Collaboration, T. Ahmed *et al.*, Z. Phys. C64 (1994) 545.

[10] H1 Collaboration, S. Aid *et al.*, Z. Phys. C71 (1996) 211.

[11] J. Butterworth and H. Dreiner, Nucl. Phys. B397 (1993) 3, and references therein.

[12] W. Buchmüller, R. Rückl and D. Wyler, Phys. Lett. B191 (1987) 442.

[13] E. Perez, "Recherche de Particules en Supersymétrie Violant la R-parité dans H1 a HERA", Doctor Degree thesis, Université Paris VI, DAPNIA/SPP report 96-1008 (in French).

[14] E. Perez and Y. Sirois, Proceed. of the Int. Workshop on Dark Matter in Astro- and Particle Physics, Heidelberg, Germany (16-20 September 1996) 615.

[15] H. Dreiner, E. Perez, Y. Sirois Proceedings Workshop "Future Physics at HERA"

[16] H1 Collaboration, "A Search for Leptoquark Bosons in DIS at High Q^2 at HERA" Contributed paper # 579 to the XXIX Int. Conf. on High Energy Physics, Vancouver, Canada (23-29 July 1998),

[17] H1 Collaboration, I. Abt *et al.*, DESY preprint 93-103 (July 1993) 194pp.; *idem* DESY Internal Report H1-96-01 (March 1996) 157pp.; *idem* Nucl. Instr. and Meth. A386 (1997) 310.

[18] H1 Calorimeter Group, B. Andrieu *et al.*, Nucl. Instr. and Meth. A336 (1993) 460.

[19] H1 Calorimeter Group, B. Andrieu *et al.*, Nucl. Inst. and Meth. A344 (1994) 492.

[20] H1 Calorimeter Group, B. Andrieu *et al.*, Nucl. Instr. and Meth. A350 (1994) 57; *idem*, Nucl. Instr. and Meth. A336 (1993) 499.

[21] H1 SPACAL Group, R.D. Appuhn *et al.*, Nucl. Instr. and Meth. A386 (1997) 397.

[22] H1 BEMC Group, J. Ban *et al.*, Nucl. Instr. and Meth. A372 (1996) 399.

[23] Ph. Bruel, Doctor Degree Thesis, Université de Paris-Sud (Orsay), "Recherche d' intéractions au-dela du Modele Standard" (in French).

[24] DJANGO 2.1; G.A. Schuler and H. Spiesberger, Proceedings of the Workshop Physics at HERA, W. Buchmüller and G. Ingelman (Editors), (October 1991, DESY-Hamburg), vol. 3 p. 1419.

[25] HERACLES 4.4; A. Kwiatkowski, H. Spiesberger and H.-J. Möhring, Comput. Phys. Commun. 69 (1992) 155.

[26] G. Gustafson and U. Pettersson, Nucl. Phys. B306 (1988) 746; *idem*, *addendum* Lund University preprint LU-TP-87-19, (October 1987) 4pp.; B. Andersson *et al.*, Z. Phys. C43 (1989) 625.

[27] ARIADNE 4.0; L. Lönnblad, Comput. Phys. Commun. 71 (1992) 15.

[28] JETSET 7.4; T. Sjöstrand, Lund Univ. preprint LU-TP-95-20 (August 1995) 321pp; *idem*, CERN preprint TH-7112-93 (February 1994) 305pp.

[29] A.D. Martin, R.G. Roberts and W.J. Stirling, Durham Univ. preprint DTP-93-86 and Rutherford Appleton Lab. preprint RAL-93-077 (October 1993) 16pp.;
(PDFLIB [30] nucleon structure function type 1, group 3, set 36) .

[30] H. Plothom-Besch, CERN-PPE Parton Density Functions program W5051.

[31] PYTHIA 5.7; T. Sjöstrand, CERN-TH-6488 (1992), Comp. Phys. Comm. 82 (1994) 74.

[32] M. Glück, E. Reya and A. Vogt, Phys. Rev. D45 (1992) 3986; *idem*, Phys. Rev. D46 (1992) 1973; (PDFLIB [30] nucleon structure function type 1, group 5 set 4; photon structure function type 3 group 5 set 3).

[33] LEGO 0.02 and SUSSEX 1.5; K. Rosenbauer, Doktor Dissertation, RWTH Aachen (in German), PITHA 95/16 (July 1995).

[34] H1 Collaboration, I. Abt *et al.*, Nucl. Phys. B396 (1993) 3; *idem*, T. Ahmed *et al.*, Z. Phys. C64 (1994) 545; *idem*, T. Ahmed *et al.*, Phys. Lett. B369 (1996) 173.

[35] S. Katsanevas, P. Morawitz, "SUSYGEN 2.2: A Monte Carlo Event Generator for MSSM sparticle production at e^+e^- colliders", hep-ph/9711417, 68pp.

[36] $D\emptyset$ Collaboration, "Search for R-parity Violating Supersymmetry in the Dielectron and Multijet Channel" Contributted paper #588 to the XXIX Int. Conf. on High Energy Physics, Vancouver, Canada (23-29 July 1998); see also http://www-d0.fnal.gov/public/new/analyses/rpareejjjj/welcome.html

[37] M. Chertok, for $D\emptyset$ and CDF Collaborations, to be published in the Proceed. of the 33^{rd} Rencontres de Moriond, QCD and High Energy Hadronic Interactions, Les Arcs, France, (March 21-28, 1998).

[38] R. Mohapatra, Phys. Rev. D34 (1986) 3457; J.D. Vergados, Phys. Lett. B184 (1987) 55.;
M. Hirsch, H.V. Klapdor-Kleingrothaus, S.G. Kovalenko, Phys. Lett. B352 (1995) 1.
M. Hirsch, H.V. Klapdor-Kleingrothaus, S.G. Kovalenko, Phys. Rev. Lett. 75 (1995) 17; Phys. Rev. D53 (1996) 1239.

[39] P. Langacker, Phys. Lett. B256 (1991) 277.

[40] J.E. Kim and P. Ko, Phys. Rev. D57 (1998) 489;

[41] H. Dreiner, to be published in "Perspectives on Supersymmetry", Ed. G.L. Kane, World Scientific, hep-ph/9707435, 18pp.

[42] Particle Data Group, Phys. Rev. D54 (1996)

[43] C.S. Wood *et al.*, Science 275 (1997) 1759.

[44] H1 Collaboration, Phys. Lett. B369 (1996) 173.

[45] ZEUS Collaboration, M. Derrick *et al.*, Z. Phys. C73 (1997) 613.

[46] CDF Collaboration, F. Abe *et al.*, Phys. Rev. Lett. 78 (1997) 2906.

[47] D$\emptyset$ Collaboration, B. Abbott *et al.*, FERMILAB preprint PUB-98-081-E (March 1998) 6pp.; eprint hep-ex/9803009.

[48] S. Davidson, D. Bailey and B. Campbell, Z. Phys. C61 (1994) 613.